

Splitting of elliptic flow in non-central relativistic heavy-ion collisions

Zhengyu Chen¹, Zeyan Wang¹, Carsten Greiner², Zhe Xu¹

¹ *Department of Physics, Tsinghua University and Collaborative Innovation Center of Quantum Matter, Beijing 100084, China and*

² *Institut für Theoretische Physik, Johann Wolfgang Goethe-Universität Frankfurt, Max-von-Laue-Strasse 1, 60438 Frankfurt am Main, Germany*

(Dated: October 18, 2021)

We predict a new effect due to the presence of the global vorticity in non-central relativistic heavy-ion collisions, namely a splitting of the elliptic flow parameter v_2 at non-zero rapidity. The size of the splitting is proposed as a new observable that can be used to constrain the initial vortical configuration of the produced QCD matter in experiments. The new findings are demonstrated by numerical calculations employing the parton cascade model, Boltzmann Approach of MultiParton Scatterings (BAMPS), for non-central Au + Au collisions at $\sqrt{s_{NN}} = 200 \text{ GeV}$.

Global spin polarization of hadrons, observed in non-central relativistic heavy-ion collisions at the BNL Relativistic Heavy Ion Collider (RHIC) and the CERN Large Hadron Collider (LHC) [1–5], indicates the generation of a strong vorticity field. The magnitude of the global vorticity is estimated to be $\omega \approx 10^{22} \text{ s}^{-1}$ [1], which is the highest value known in nature. Such strong vorticity opens a new window for the study of the quark-gluon plasma (QGP) in heavy-ion collisions. Theoretical developments such as spin kinetic theory [6–15] and spin hydrodynamics [16–21] become new interdisciplinary research areas.

Current studies are focusing on the initial vortical configuration of the QCD matter in non-central heavy-ion collisions. The directed flow v_1 of the light charged hadrons [22–24] and heavy flavor hadrons [25–28] are suggested as probes to the initial tilted shape of matter. Still, there exists a spin sign problem [29–31] between the experimental and theoretical results on the local polarization such as azimuthal angle dependence, which demands deeper understanding to the initial vortical configuration. In this Letter, we predict a new effect of the global vorticity and propose a new observable, which can be used to constrain the initial vortical configuration of matter.

The idea comes from the thought of a possible effect of the vortical motion on the expansion transversely to the beam axis. For a rigid rotating plasma, the authors in Ref. [32] found an enhancement of the elliptic flow v_2 due to the centrifugal effect. However, since the equation of state (EOS) of QGP is very soft, the global orbital angular momentum would probably never result in a rigid rotation of the produced QCD matter. Instead, it will give rise to the shear of the longitudinal flow, which leads to a collective motion round the y axis in addition to the longitudinal expansion along the beam (z) axis and the transverse expansion in the $x - y$ plane. The shape of the expanding matter in the reaction plane is sketched in Fig. 1 (d), compared to the case without the vortical behavior [see Fig. 1 (c)]. It seems that the vortical motion will “drive” the system outwards in the I and III quadrant and “press” the system inwards in the II and IV quadrant. Thus, the vortical motion breaks the mirror

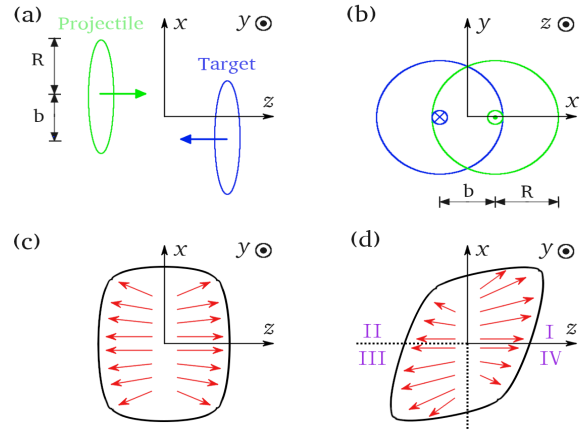


FIG. 1. A sketch of the collective motion of the QCD matter produced in a non-central relativistic heavy-ion collision.

symmetry with regards to the $y - z$ plane and also the Bjorken boost invariance, which hold in the case without the vortical motion. Considering a particular piece at a space-time rapidity η_s , namely the medium in the $x - y$ plane at a certain $\eta_s = 1/2 \ln(t + z)/(t - z)$. Due to the symmetry breaking at non-zero η_s , the collective expansion in the half $x - y$ plane with positive x is different from that in the another half plane with negative x . This difference may be transferred into the final particle momentum distribution. From this thought we predict that the elliptic flow parameter v_2 at non-zero momentum rapidity measured using particles with positive p_x is different from that v_2 measured using particles with negative p_x . We call this the splitting of the elliptic flow. In the following we will demonstrate the new finding by calculations within kinetic theory.

We employ the Monte Carlo kinetic transport model, Boltzmann Approach of MultiParton Scatterings (BAMPS)[33, 34], to calculate the space-time evolution of the quark gluon matter in heavy-ion collisions. BAMPS had successfully described the experimental data of elliptic flow measured at RHIC and LHC [35–37].

Now we briefly present the initial condition for subse-

quent kinetic transport calculations shown later in this letter. In the Glauber picture of heavy-ion collisions, quarks and gluons are initially produced in “hard” binary nucleon-nucleon collisions as well as in “soft” collective collisions between participant nucleons of the projectile and target nucleus. The latter can be described in the wounded nucleon model [38], in which the number of produced quarks and gluons is assumed to be proportional to the number of participant nucleons and the quarks and gluons will take a part of the momentum of the participant projectile and target nucleons. Due to the unequal local number densities of participant projectile and target nucleons, the quark gluon system possesses a global angular momentum round the y axis.

The participant nucleon number distribution in the transverse plane can be evaluated as [38]

$$\frac{dN_{part}^{P,T}}{d\mathbf{x}_T} = T^{P,T}(\mathbf{x}_T, b) \{1 - \exp[-\sigma_{p+p} T^{T,P}(\mathbf{x}_T, b)]\} \quad (1)$$

where the superscript P or T denotes projectile or target, σ_{p+p} is the nucleon-nucleon reaction cross section, which is approximately 42 mb for Au+Au collisions at top RHIC energy, and

$$T^{P,T}(\mathbf{x}_T, b) = \int dz n_{WS}^{P,T}(\mathbf{x}_T, z, b) \quad (2)$$

is the thickness function of the projectile (target) nucleus. Here $n_{WS}^{P,T}(\mathbf{x}_T, z, b)$ is the Woods-Saxon distribution for the nuclear density of the colliding nucleus. The participant nucleon number relative asymmetry distribution is defined as

$$A_{part}(\mathbf{x}_T, b) = \frac{dN_{part}^P/d\mathbf{x}_T - dN_{part}^T/d\mathbf{x}_T}{dN_{part}^P/d\mathbf{x}_T + dN_{part}^T/d\mathbf{x}_T}. \quad (3)$$

In the BAMPS calculations performed before [37], the initial condition was the production of quarks and gluons according to the “hard” nucleon-nucleon binary collisions. The “soft” particle production from the wounded participant nucleons, which is essential for the global vorticity, was neglected. When calculating the total angular momentum \mathbf{J} by

$$\mathbf{J} = \sum_i \mathbf{r}_i \times \mathbf{p}_i, \quad (4)$$

where \mathbf{r}_i and \mathbf{p}_i are the position and momentum of i -th particle, we find that the default initialization leads to zero orbital angular momentum because of the mirror symmetry with regards to the $y - z$ plane [see Fig. 1 (c)]. To consider an orbital angular momentum in the present study, we will modify the default initialization instead of adding the “soft” particle production. To be specific, we randomly choose $1/5$ of the particles from the default initialization and treat them as if they were produced from the wounded nucleons. To give these particles a global orbital angular momentum, we randomly

choose such particles at positive (negative) x with negative (positive) p_z and change the sign of p_z , so that the asymmetry between particles with positive and negative p_z is equal to $A_{part}(\mathbf{x}_T, b)/5$, namely,

$$\frac{dN_+/d\mathbf{x}_T - dN_-/d\mathbf{x}_T}{dN/d\mathbf{x}_T} = \frac{1}{5} A_{part}(\mathbf{x}_T, b), \quad (5)$$

where N_+ (N_-) denotes the number of particles with positive (negative) p_z and $N = N_+ + N_-$. Let W be the probability for changing the sign of p_z of a certain particle. For instance, some particles at positive x with negative p_z will change their sign to be positive. The average number of those particles is obviously $\frac{1}{2}dN/d\mathbf{x}_T W$. Thus, we have $dN_-/d\mathbf{x}_T = \frac{1}{2}dN/d\mathbf{x}_T(1 - W)$ and $dN_+/d\mathbf{x}_T = \frac{1}{2}dN/d\mathbf{x}_T(1 + W)$. Putting these relations in Eq. (5) gives $W = A_{part}(\mathbf{x}_T, b)/5$, with which we modify the default initialization. The modification leads to $J_y = 1.4 \times 10^4 \hbar$ for Au+Au collisions at top RHIC energy $\sqrt{s_{NN}} = 200 \text{ GeV}$ with impact parameter $b = 7 \text{ fm}$. This is $5 - 7$ times smaller than the result from AMPT model [39] and the analytical result from [40], and is almost the same as the result from HIJING model [41] and from the recent work [28]. Figure 2 shows the profile of the initial longitudinal velocities of sheets transverse to x axis, where $v_z = \sum_i p_{iz} / \sum_i E_i$. The sum is over particles from all rapidity in a small Δx window.

After the initialization, the space-time evolution and collisions of quarks and gluons are calculated by BAMPS. All $2 \leftrightarrow 2$ and $2 \leftrightarrow 3$ pQCD processes for gluons and u , d , and s quarks are included. The details of the implementation can be found in [37]. We did some improvements for the present study. The test particle number N_{test} is increased from 250 to 25000 to get higher statistics. The cell length in the transverse plane is reduced from $dx = dy = 0.4 \text{ fm}$ to 0.05 fm . The cell length in the space-time rapidity is about $d\eta_s \approx 0.02$ and almost unchanged. The local quantities such as the par-

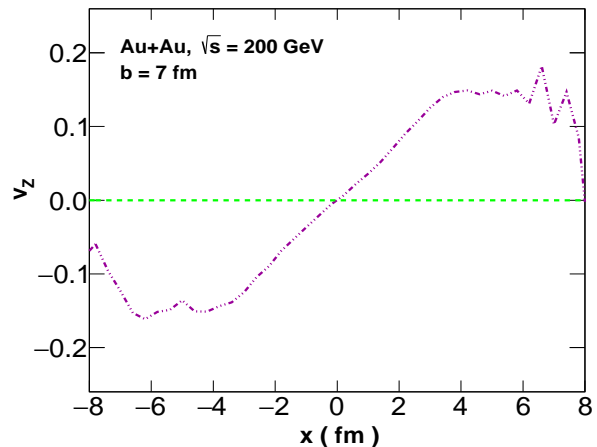


FIG. 2. Longitudinal velocity profile along x axis from the modified initialization for a Au + Au collision at top RHIC energy $\sqrt{s_{NN}} = 200 \text{ GeV}$ with impact parameter $b = 7 \text{ fm}$.

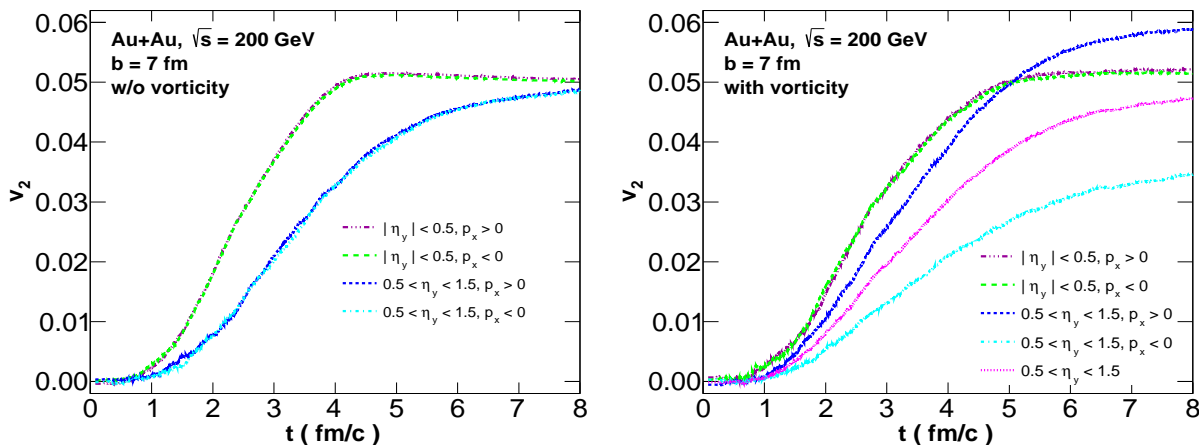


FIG. 3. Time evolution of the elliptic flow v_2 from BAMPS calculations for Au+Au collisions at $\sqrt{s_{NN}} = 200$ GeV with $b = 7$ fm. v_2 is evaluated for particles at mid-rapidity and higher rapidity with positive or negative p_x . The left panel shows the results with the default initialization without a global vorticity, whereas the right panel shows the results with the modified initialization with a global vorticity.

ticle number and energy density, Debye mass, and the mean-free path etc., which are needed to determine the transition cross-sections and the freeze-out condition, are calculated locally in a small box with $dx = dy = 0.4$ fm and $d\eta_s \approx 0.02$. Other setups are the same as made in [37].

In the following we show the numerical results from BAMPS calculations for Au+Au collisions at top RHIC energy $\sqrt{s_{NN}} = 200$ GeV with $b = 7$ fm. The initial condition is either the default initialization with zero \mathbf{J} or the modified one with non-zero \mathbf{J} , in order to demonstrate the significance of a global vorticity.

We calculate the elliptic flow parameter v_2 in two rapidity windows. Here the momentum rapidity is defined as $\eta_y = 1/2 \ln[(E + p_z)/(E - p_z)]$. The two rapidity windows are chosen at mid-rapidity $[-0.5 : 0.5]$ and higher rapidity $[0.5 : 1.5]$. v_2 is evaluated by $v_2 = \sum_i (p_{ix}^2 - p_{iy}^2) / (p_{ix}^2 + p_{iy}^2)$, where the sum is over the particles with positive p_x , or the particles with negative p_x , or all the particles in the given rapidity window, respectively.

Figure 3 shows the buildup of v_2 . The left panel depicts the results with the default initialization, whereas the right panel depicts the results with the modified initialization. We see no difference between v_2 for particles with positive p_x and that for particles with negative p_x in both rapidity windows for the default initialization without a global vorticity, as it should be due to the mirror symmetry with regards to the $y - z$ plane, see Fig. 1 (c). The mirror symmetry is broken for the modified initialization with a global vorticity, see Fig. 1 (d). However, the symmetry between the distribution at rapidity η_y and that at $-\eta_y$ by changing p_x to $-p_x$ holds. This is the reason that v_2 of particles with positive p_x in the mid-rapidity window $[-0.5 : 0.5]$ is the same as that for particles with negative p_x for the modified initialization. It is not the case for v_2 in the higher rapidity

window $[0.5 : 1.5]$, because the Bjorken boost invariance is not valid any more due to the global vorticity. We see that at the higher positive rapidity the v_2 of particles with positive p_x is much larger than that of particles with negative p_x for the modified initialization, although the v_2 for all particles, depicted by the red curve in the right panel of Fig. 3, is only a little smaller than that for the default initialization. We call this new finding the splitting of the elliptic flow at non-zero rapidity in presence of a global vorticity. The splitting is also seen in the p_T dependence of v_2 at the final time, as shown in the right panel of Fig. 4. When comparing the results with and without the vorticity in Fig. 4, we see that the vortical motion shifts the curve of $p_x > 0$ up and shifts the one of $p_x < 0$ down. Note that the hadronization and the hadronic interactions are not included in the present BAMPS calculations. The hadronic p_T dependence would be higher at intermediate p_T due to the quark recombination. Nevertheless, the splitting effect would remain in a full transport calculation.

As mentioned before and illustrated in Fig. 1 (d), the global vorticity seems to “drive” the system outwards in quadrant I and to “press” the system inwards in quadrant IV. Therefore, qualitatively, the vorticity will enhance the transverse flow in quadrant I and reduce the transverse flow in quadrant IV. In other words, the vorticity will cause an additional flow in quadrant I and an antflow in quadrant IV. This is the reason why at positive rapidity the v_2 of particles with positive p_x is always larger than that of particles with negative p_x .

We note that the initial fluctuation was not taken into account in the initial particle distribution for BAMPS calculations. The pure initial fluctuation may also lead to the splitting of the elliptic flow. Whether v_2 of particles with positive p_x is larger or smaller than that of particles with negative p_x , is random on the event by event basis. This is different from the vorticity induced splitting.

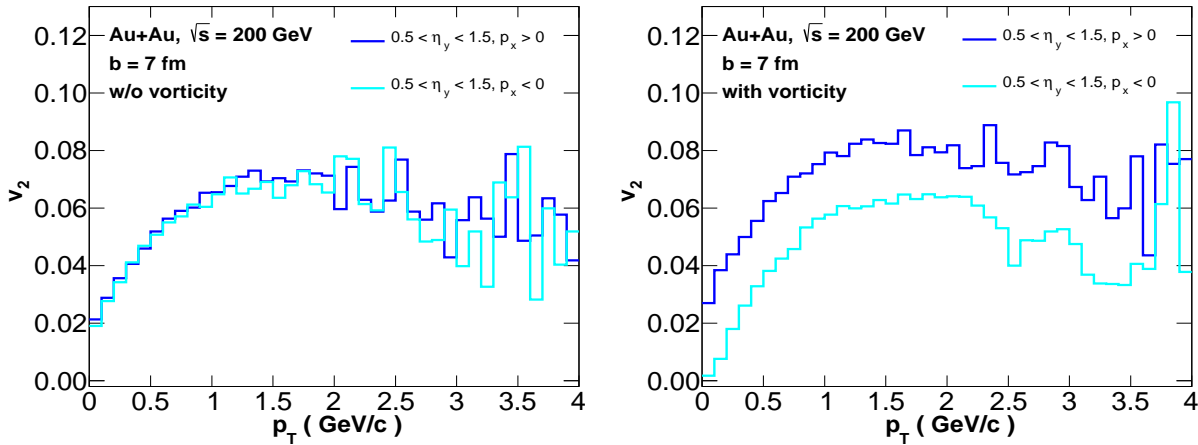


FIG. 4. Same as Fig. 3, but for the p_T dependence of the final v_2 in the rapidity window $[0.5 : 1.5]$.

The sizable splitting of the elliptic flow, shown in Figs. 3 and 4 from our calculations, serves as a demonstration of the significance of the global vorticity. When decreasing the number of the “soft” particles in the initialization to be 1/10 of all particles, (instead of 1/5 used), the global orbital angular momentum is decreased to $J_y = 0.63 \times 10^4 \hbar$ and the initial profile of the longitudinal velocity becomes less steep than that shown in Fig. 2. For this initial condition, the size of the splitting of the elliptic flow at the final time is about 0.014, which is smaller than the value of 0.024 taken from Fig. 3. Qualitatively, the larger the global orbital angular momentum, and/or the more pronounced the initial vortical configuration, and/or the smaller the shear viscosity, the more significant is the splitting of the elliptic flow. To make these dependence clear, further theoretical investigations are needed. From the experimental side, a confirmation of the splitting of the elliptic flow by experimental measurements could prove the existence of a global vorticity and the measured size of the splitting could be used to constrain the vortical configuration in the early stage of heavy-ion collisions.

In summary, we have studied the possible experimental significance of a global vorticity in non-central relativistic heavy-ion collisions and proposed the splitting of the elliptic flow at non-zero rapidity as a new measurable observable. The idea is repeated here. The collective motion of a global vorticity will break the mirror symmetry with regards to the $y - z$ plane and the Bjorken boost invariance, which hold in the case without a global vorticity. The difference in the motion above and under the $y - z$ plane in the coordinate space can be transferred into the momentum space, which makes a splitting of the elliptic flow parameter v_2 at non-zero rapidity with regards to the sign of p_x . By employing the parton cascade model BAMPS for the default and modified initialization

of quarks and gluons in a Au + Au collision at RHIC energy $\sqrt{s_{NN}} = 200 \text{ GeV}$ with impact parameter $b = 7 \text{ fm}$, we obtained a significant splitting of the elliptic flow v_2 in the rapidity window $[0.5 : 1.5]$, when a global vorticity is present.

We have to note that since the particle distribution function is given in Fourier-series,

$$\frac{dN}{d^2p_T d\eta_y} = \frac{dN}{2\pi p_T dp_T d\eta_y} \left\{ 1 + 2 \sum_n v_n \cos[n(\psi - \Psi_n)] \right\}, \quad (6)$$

the splitting of v_2 , Δv_2 , can be mathematically expressed by all v_n and Ψ_n . In particular, all even v_n and Ψ_n disappear. If higher order flow parameters can be neglected, we have approximately $\Delta v_2 \approx (8/3\pi)v_1 \cos(\Psi_2 - \Psi_1)$. v_1 and $\Psi_2 - \Psi_1$ fluctuate event-by-event. We see that Δv_2 and v_1 have the same sign. Qualitative analysis as well as numerical calculations presented in this study show that the defined Δv_2 at positive rapidity is positive. However, the measured v_1 [22, 42–44] is negative at positive rapidity. This may be due to the contribution of non-flow effects to the particle distribution function. It seems that v_1 is not completely equivalent to Δv_2 that we proposed. Since non-flow effects have been already handled in data analyses for v_2 measurements, we suggest the observation of the splitting effect of the elliptic flow in experiments.

The authors would like to thank Pengfei Zhuang and Dariusz Miskowiec for fruitful discussions. This work was financially supported by the National Natural Science Foundation of China under Grants No. 11890710, No. 11890712, and No. 12035006. C.G. acknowledges support by the Deutsche Forschungsgemeinschaft (DFG) through the grant CRC-TR 211 “Strong-interaction matter under extreme conditions”. The BAMPS simulations were performed at Tsinghua National Laboratory for Information Science and Technology and on TianHe-1(A) at National Supercomputer Center in Tianjin.

- [1] L. Adamczyk *et al.* [STAR], *Nature* **548**, 62-65 (2017) doi:10.1038/nature23004 [arXiv:1701.06657 [nucl-ex]].
- [2] J. Adam *et al.* [STAR], *Phys. Rev. C* **98**, 014910 (2018) doi:10.1103/PhysRevC.98.014910 [arXiv:1805.04400 [nucl-ex]].
- [3] B. I. Abelev *et al.* [STAR], *Phys. Rev. C* **76**, 024915 (2007) [erratum: *Phys. Rev. C* **95**, no.3, 039906 (2017)] doi:10.1103/PhysRevC.76.024915 [arXiv:0705.1691 [nucl-ex]].
- [4] B. I. Abelev *et al.* [STAR], *Phys. Rev. C* **77**, 061902 (2008) doi:10.1103/PhysRevC.77.061902 [arXiv:0801.1729 [nucl-ex]].
- [5] S. Acharya *et al.* [ALICE], *Phys. Rev. Lett.* **125**, no.1, 012301 (2020) doi:10.1103/PhysRevLett.125.012301 [arXiv:1910.14408 [nucl-ex]].
- [6] D. L. Yang, *Phys. Rev. D* **98**, no.7, 076019 (2018) doi:10.1103/PhysRevD.98.076019 [arXiv:1807.02395 [nucl-th]].
- [7] N. Mueller and R. Venugopalan, *Phys. Rev. D* **99**, no.5, 056003 (2019) doi:10.1103/PhysRevD.99.056003 [arXiv:1901.10492 [hep-th]].
- [8] N. Weickgenannt, X. L. Sheng, E. Speranza, Q. Wang and D. H. Rischke, *Phys. Rev. D* **100**, no.5, 056018 (2019) doi:10.1103/PhysRevD.100.056018 [arXiv:1902.06513 [hep-ph]].
- [9] J. H. Gao and Z. T. Liang, *Phys. Rev. D* **100**, no.5, 056021 (2019) doi:10.1103/PhysRevD.100.056021 [arXiv:1902.06510 [hep-ph]].
- [10] K. Hattori, Y. Hidaka and D. L. Yang, *Phys. Rev. D* **100**, no.9, 096011 (2019) doi:10.1103/PhysRevD.100.096011 [arXiv:1903.01653 [hep-ph]].
- [11] Z. Wang, X. Guo, S. Shi and P. Zhuang, *Phys. Rev. D* **100**, no.1, 014015 (2019) doi:10.1103/PhysRevD.100.014015 [arXiv:1903.03461 [hep-ph]].
- [12] S. Li and H. U. Yee, *Phys. Rev. D* **100**, no.5, 056022 (2019) doi:10.1103/PhysRevD.100.056022 [arXiv:1905.10463 [hep-ph]].
- [13] D. L. Yang, K. Hattori and Y. Hidaka, *JHEP* **07**, 070 (2020) doi:10.1007/JHEP07(2020)070 [arXiv:2002.02612 [hep-ph]].
- [14] Y. C. Liu, K. Mameda and X. G. Huang, *Chin. Phys. C* **44**, no.9, 094101 (2020) doi:10.1088/1674-1137/44/9/094101 [arXiv:2002.03753 [hep-ph]].
- [15] S. Bhadury, W. Florkowski, A. Jaiswal, A. Kumar and R. Ryblewski, *Phys. Lett. B* **814**, 136096 (2021) doi:10.1016/j.physletb.2021.136096 [arXiv:2002.03937 [hep-ph]].
- [16] W. Florkowski, B. Friman, A. Jaiswal and E. Speranza, *Phys. Rev. C* **97**, no.4, 041901 (2018) doi:10.1103/PhysRevC.97.041901 [arXiv:1705.00587 [nucl-th]].
- [17] W. Florkowski, A. Kumar and R. Ryblewski, *Phys. Rev. C* **98**, no.4, 044906 (2018) doi:10.1103/PhysRevC.98.044906 [arXiv:1806.02616 [hep-ph]].
- [18] D. Montenegro and G. Torrieri, *Phys. Rev. D* **100**, no.5, 056011 (2019) doi:10.1103/PhysRevD.100.056011 [arXiv:1807.02796 [hep-th]].
- [19] K. Hattori, M. Hongo, X. G. Huang, M. Matsuo and H. Taya, *Phys. Lett. B* **795**, 100-106 (2019) doi:10.1016/j.physletb.2019.05.040 [arXiv:1901.06615 [hep-th]].
- [20] K. Fukushima and S. Pu, *Phys. Lett. B* **817**, 136346 (2021) doi:10.1016/j.physletb.2021.136346 [arXiv:2010.01608 [hep-th]].
- [21] S. Li, M. A. Stephanov and H. U. Yee, *Phys. Rev. Lett.* **127**, no.8, 082302 (2021) doi:10.1103/PhysRevLett.127.082302 [arXiv:2011.12318 [hep-th]].
- [22] L. Adamczyk *et al.* [STAR], *Phys. Rev. Lett.* **112**, no.16, 162301 (2014) doi:10.1103/PhysRevLett.112.162301 [arXiv:1401.3043 [nucl-ex]].
- [23] P. Bozek and I. Wyskiel, *Phys. Rev. C* **81**, 054902 (2010) doi:10.1103/PhysRevC.81.054902 [arXiv:1002.4999 [nucl-th]].
- [24] Y. Nara, H. Niemi, A. Ohnishi and H. Stöcker, *Phys. Rev. C* **94**, no.3, 034906 (2016) doi:10.1103/PhysRevC.94.034906 [arXiv:1601.07692 [hep-ph]].
- [25] J. Adam *et al.* [STAR], *Phys. Rev. Lett.* **123**, no.16, 162301 (2019) doi:10.1103/PhysRevLett.123.162301 [arXiv:1905.02052 [nucl-ex]].
- [26] S. Chatterjee and P. Bozek, *Phys. Rev. Lett.* **120**, no.19, 192301 (2018) doi:10.1103/PhysRevLett.120.192301 [arXiv:1712.01189 [nucl-th]].
- [27] B. Chen, M. Hu, H. Zhang and J. Zhao, *Phys. Lett. B* **802**, 135271 (2020) doi:10.1016/j.physletb.2020.135271 [arXiv:1910.08275 [nucl-th]].
- [28] L. Oliva, S. Plumari and V. Greco, *JHEP* **05**, 034 (2021) doi:10.1007/JHEP05(2021)034 [arXiv:2009.11066 [hep-ph]].
- [29] F. Becattini and M. A. Lisa, *Ann. Rev. Nucl. Part. Sci.* **70**, 395-423 (2020) doi:10.1146/annurev-nucl-021920-095245 [arXiv:2003.03640 [nucl-ex]].
- [30] J. H. Gao, G. L. Ma, S. Pu and Q. Wang, *Nucl. Sci. Tech.* **31**, no.9, 90 (2020) doi:10.1007/s41365-020-00801-x [arXiv:2005.10432 [hep-ph]].
- [31] Y. C. Liu and X. G. Huang, *Nucl. Sci. Tech.* **31**, no.6, 56 (2020) doi:10.1007/s41365-020-00764-z [arXiv:2003.12482 [nucl-th]].
- [32] F. Becattini, F. Piccinini and J. Rizzo, *Phys. Rev. C* **77**, 024906 (2008) doi:10.1103/PhysRevC.77.024906 [arXiv:0711.1253 [nucl-th]].
- [33] Z. Xu and C. Greiner, *Phys. Rev. C* **71**, 064901 (2005) doi:10.1103/PhysRevC.71.064901 [arXiv:hep-ph/0406278 [hep-ph]].
- [34] Z. Xu and C. Greiner, *Phys. Rev. C* **76**, 024911 (2007) doi:10.1103/PhysRevC.76.024911 [arXiv:hep-ph/0703233 [hep-ph]].
- [35] Z. Xu, C. Greiner and H. Stöcker, *Phys. Rev. Lett.* **101**, 082302 (2008) doi:10.1103/PhysRevLett.101.082302 [arXiv:0711.0961 [nucl-th]].
- [36] Z. Xu and C. Greiner, *Phys. Rev. C* **79**, 014904 (2009) doi:10.1103/PhysRevC.79.014904 [arXiv:0811.2940 [hep-ph]].
- [37] J. Uphoff, F. Senzel, O. Fochler, C. Wesp, Z. Xu and C. Greiner, *Phys. Rev. Lett.* **114**, no.11, 112301 (2015) doi:10.1103/PhysRevLett.114.112301 [arXiv:1401.1364 [hep-ph]].
- [38] M. L. Miller, K. Reygers, S. J. Sanders and P. Steinberg, *Ann. Rev. Nucl. Part. Sci.* **57**, 205-

- 243 (2007) doi:10.1146/annurev.nucl.57.090506.123020 [arXiv:nucl-ex/0701025 [nucl-ex]].
- [39] Y. Jiang, Z. W. Lin and J. Liao, Phys. Rev. C **94**, no.4, 044910 (2016) [erratum: Phys. Rev. C **95**, no.4, 049904 (2017)] doi:10.1103/PhysRevC.94.044910 [arXiv:1602.06580 [hep-ph]].
- [40] J. H. Gao, S. W. Chen, W. t. Deng, Z. T. Liang, Q. Wang and X. N. Wang, Phys. Rev. C **77**, 044902 (2008) doi:10.1103/PhysRevC.77.044902 [arXiv:0710.2943 [nucl-th]].
- [41] W. T. Deng and X. G. Huang, Phys. Rev. C **93**, no.6, 064907 (2016) doi:10.1103/PhysRevC.93.064907 [arXiv:1603.06117 [nucl-th]].
- [42] B. B. Back *et al.* [PHOBOS], Phys. Rev. Lett. **97**, 012301 (2006) doi:10.1103/PhysRevLett.97.012301 [arXiv:nucl-ex/0511045 [nucl-ex]].
- [43] J. Adams *et al.* [STAR], Phys. Rev. C **73**, 034903 (2006) doi:10.1103/PhysRevC.73.034903 [arXiv:nucl-ex/0510053 [nucl-ex]].
- [44] B. I. Abelev *et al.* [STAR], Phys. Rev. Lett. **101**, 252301 (2008) doi:10.1103/PhysRevLett.101.252301 [arXiv:0807.1518 [nucl-ex]].